arXiv:1611.10155v1 [hep-ph] 30 Nov 2016

MCNET-16-45
December 1, 2016

# Top and Electroweak bosons and Higgs

Eleni Vryonidou[1]

*Centre for Cosmology, Particle Physics and Phenomenology (CP3), Université catholique de Louvain, B-1348 Louvain-la-Neuve, Belgium*
*and*
*Nikhef Theory Group, Science Park 105, 1098 XG Amsterdam, The Netherlands*

In this talk I review recent progress in the computation of processes involving top quarks in the framework of Standard Model Effective Theory at NLO in QCD. In particular I discuss the impact of higher-dimensional operators on top pair production in association with a photon, a $Z$ boson and a Higgs. Results are obtained within the automated framework of MadGraph5_aMC@NLO.

PRESENTED AT

$9^{th}$ International Workshop on Top Quark Physics
Olomouc, Czech Republic, September 19–23, 2016

[1]Work supported by the European Union as part of the FP7 Marie Curie Initial Training Network MCnetITN (PITN-GA-2012-315877).

# 1 Introduction

With Run-II of the LHC, a plethora of precise top-quark measurements is expected. In addition to the main production processes: pair and single top production, results for the associated production of top quarks with a vector boson and a Higgs have been collected by CMS and ATLAS. Remarkable progress has been achieved in providing precise theoretical predictions for this class of processes in the Standard Model (SM). In particular the $t\bar{t}H$ process is known at next-to-leading order (NLO) in QCD [1–4], with off-shell effects [5], and at NLO in electroweak (EW) [6, 7]. Results for $t\bar{t}Z$ have been presented at NLO in QCD in [3, 8] and NLO in EW in [6], while $t\bar{t}\gamma$ is known at NLO in QCD [3, 9]. A detailed phenomenological study of SM top production in association with a Higgs and electroweak bosons can be found in [10].

Precise predictions for deviations from the SM will become equally important at the LHC Run II. The Standard Model Effective Field Theory (SMEFT) provides a powerful framework to consistently and systematically describe deviations from the SM via higher-dimension operators which modify the SM Lagrangian as follows:

$$\mathcal{L} = \mathcal{L}_{SM} + \sum_i \frac{C_i}{\Lambda^2} O_i + \mathcal{O}(\Lambda^{-4}). \tag{1}$$

Recently fully differential NLO QCD corrections to top-quark processes in the EFT have started to become available. These include the top-decay processes [11, 12], single-top production triggered by flavor-changing neutral interactions [13], top-quark pair production and single top production [14,15]. QCD corrections are found to have a large and nontrivial impact on both the total cross sections and the differential distributions. NLO results come with reduced theoretical uncertainties and can therefore play an important role in extracting more reliable information in the context of global EFT fits [16, 17].

In this talk I focus on the recent computation of $t\bar{t}Z$, $t\bar{t}\gamma$ and $t\bar{t}H$ at dimension-six at NLO in QCD discussed in more detail in [23, 24]. These results have become available within the MadGraph5_aMC@NLO framework [18]. FeynRules and NLOCT are used to obtain a UFO model [19–22] which is then imported into MadGraph5_aMC@NLO to provide NLO accurate results.

# 2 $t\bar{t}Z/\gamma$ in the EFT

The operators contributing to $t\bar{t}Z/\gamma$ production up to dimension-six are the following [25, 26]:

$$\begin{aligned} O_{\varphi Q}^{(3)} &= i\tfrac{1}{2}y_t^2 \left(\varphi^\dagger \overleftrightarrow{D}^I_\mu \varphi\right)(\overline{Q}\gamma^\mu \tau^I Q), \;\; O_{\varphi Q}^{(1)} = i\tfrac{1}{2}y_t^2 \left(\varphi^\dagger \overleftrightarrow{D}_\mu \varphi\right)(\overline{Q}\gamma^\mu Q) \\ O_{\varphi t} &= i\tfrac{1}{2}y_t^2 \left(\varphi^\dagger \overleftrightarrow{D}_\mu \varphi\right)(\bar{t}\gamma^\mu t), \;\; O_{tW} = y_t g_w (\overline{Q}\sigma^{\mu\nu}\tau^I t)\tilde{\varphi} W^I_{\mu\nu} \\ O_{tB} &= y_t g_Y (\overline{Q}\sigma^{\mu\nu} t)\tilde{\varphi} B_{\mu\nu} \;\text{ and }\; O_{tG} = y_t g_s (\overline{Q}\sigma^{\mu\nu} T^A t)\tilde{\varphi} G^A_{\mu\nu}\,. \end{aligned} \tag{2}$$

| 13TeV | $\mathcal{O}_{tG}$ | $\mathcal{O}_{\phi Q}^{(3)}$ | $\mathcal{O}_{\phi t}$ | $\mathcal{O}_{tW}$ |
|---|---|---|---|---|
| $\sigma_{i,LO}^{(1)}$ | $286.7^{+38.2\%}_{-25.5\%}$ | $78.3^{+40.4\%}_{-26.6\%}$ | $51.6^{+40.1\%}_{-26.4\%}$ | $-0.20^{+88.0\%}_{-230.0\%}$ |
| $\sigma_{i,NLO}^{(1)}$ | $310.5^{+5.4\%}_{-9.7\%}$ | $90.6^{+7.1\%}_{-11.0\%}$ | $57.5^{+5.8\%}_{-10.3\%}$ | $-1.7^{+31.3\%}_{-49.1\%}$ |
| $K$-factor | 1.08 | 1.16 | 1.11 | 8.5 |
| $\sigma_{ii,LO}^{(2)}$ | $258.5^{+49.7\%}_{-30.4\%}$ | $2.8^{+39.7\%}_{-26.9\%}$ | $2.9^{+39.7\%}_{-26.7\%}$ | $20.9^{+44.3\%}_{-28.3\%}$ |
| $\sigma_{ii,NLO}^{(2)}$ | $244.5^{+4.2\%}_{-8.1\%}$ | $3.8^{+13.2\%}_{-14.4\%}$ | $3.9^{+13.8\%}_{-14.6\%}$ | $24.2^{+6.2\%}_{-11.2\%}$ |
| $K$-factor | 0.95 | 1.4 | 1.3 | 1.2 |

Table 1: Cross sections (in fb) and corresponding $K$-factors for $t\bar{t}Z$ production at the LHC at $\sqrt{s} = 13$ TeV for the different dimension-six operators. Percentages correspond to scale uncertainties.

The above operators form a complete set that parameterises the top-quark interactions to the gluon and the electroweak gauge bosons, which contribute at $\mathcal{O}(\Lambda^{-2})$. The contributions of these operators to $t\bar{t}Z$, $t\bar{t}\gamma$ and $t\bar{t}\mu^+\mu^-$ are computed in [23] at NLO in QCD. As an example we show results for $t\bar{t}Z$ in Table 1, where the following notation is used:

$$\sigma = \sigma_{SM} + \sum_i \frac{C_i}{(\Lambda/1\text{TeV})^2}\sigma_i^{(1)} + \sum_{i\leq j} \frac{C_i C_j}{(\Lambda/1\text{TeV})^4}\sigma_{ij}^{(2)} \,. \tag{3}$$

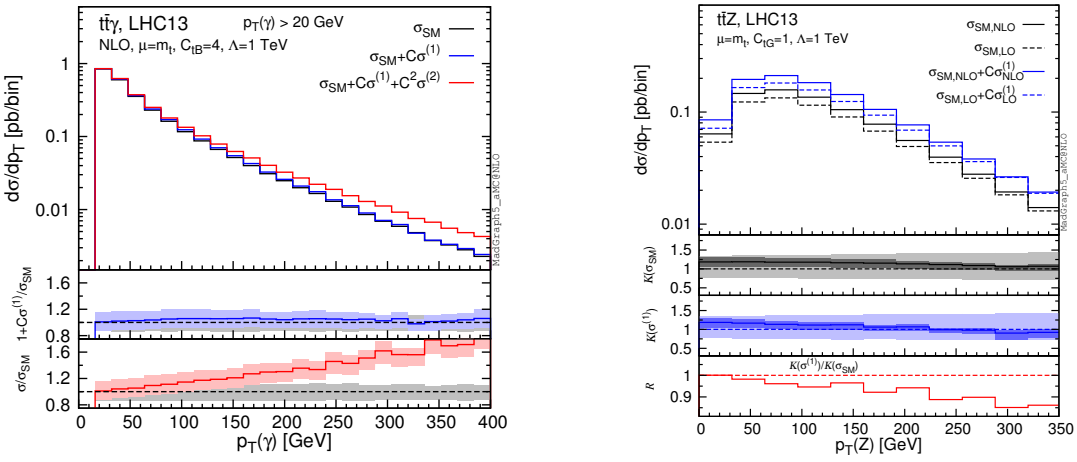


Figure 1: Left: $p_T$ of the photon in $t\bar{t}\gamma$ at 13 TeV for $C_{tB} = 4, \Lambda = 1$ TeV and ratio over the SM. Right: $p_T$ of the $Z$ in $t\bar{t}Z$ for $C_{tG} = 1, \Lambda = 1$ TeV. Comparison between the SM and the interference term differential $K$-factors.

Differential distributions for $t\bar{t}Z$, $t\bar{t}\gamma$ and $t\bar{t}\mu^+\mu^-$ are also obtained in [23]. We show some representative results in Fig. 1 for the $Z$ and photon $p_T$, which demonstrate the difference between the SM and dimension-6 shapes and $K$-factors. Results for all processes are summarised in Fig. 2 which shows the contribution of the various operators to the different processes at LO and NLO. We note here that the same set of operators impacts the gluon fusion contribution to $HZ$ production and $e^+e^- \to t\bar{t}$, for which results are also presented in [23].

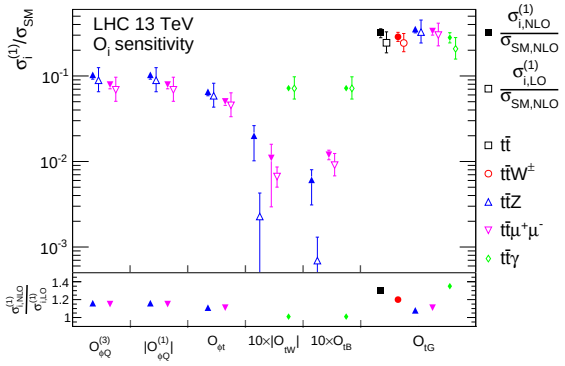


Figure 2: Sensitivity of various top quark processes to the various operators shown at LO and NLO at 13 TeV. $K$-factors are also shown for $\sigma_i^{(1)}$ as well as the scale uncertainties.

| 13 TeV | $\sigma$ NLO | $K$-factors |
|---|---|---|
| $\sigma_{SM}$ | $0.507^{+0.030+0.000+0.007}_{-0.048-0.000-0.008}$ | 1.09 |
| $\sigma_{t\phi}$ | $-0.062^{+0.006+0.001+0.001}_{-0.004-0.001-0.001}$ | 1.13 |
| $\sigma_{\phi G}$ | $0.872^{+0.131+0.037+0.013}_{-0.123-0.035-0.016}$ | 1.39 |
| $\sigma_{tG}$ | $0.503^{+0.025+0.001+0.007}_{-0.046-0.003-0.008}$ | 1.07 |
| $\sigma_{t\phi,t\phi}$ | $0.0019^{+0.0001+0.0001+0.000}_{-0.0002-0.000-0.000}$ | 1.17 |
| $\sigma_{\phi G,\phi G}$ | $1.021^{+0.204+0.096+0.024}_{-0.178-0.085-0.029}$ | 1.58 |
| $\sigma_{tG,tG}$ | $0.674^{+0.036+0.004+0.016}_{-0.067-0.007-0.019}$ | 1.04 |
| $\sigma_{t\phi,\phi G}$ | $-0.053^{+0.008+0.003+0.001}_{-0.008-0.004-0.001}$ | 1.42 |
| $\sigma_{t\phi,tG}$ | $-0.031^{+0.003+0.000+0.000}_{-0.002-0.000-0.000}$ | 1.10 |
| $\sigma_{\phi G,tG}$ | $0.859^{+0.127+0.021+0.017}_{-0.126-0.020-0.022}$ | 1.37 |

Figure 3: NLO cross sections in pb for $ttH$ at 13 TeV and corresponding $K$-factors. Scale, EFT scale and PDF uncertainties are also included.

## 3 $t\bar{t}H$ in the EFT

For $t\bar{t}H$ production we consider the following operators [24]:

$$O_{t\phi} = y_t^3 \left(\phi^\dagger\phi\right)\left(\overline{Q}t\right)\tilde{\phi}\,, \;\; O_{\phi G} = y_t^2 \left(\phi^\dagger\phi\right) G^A_{\mu\nu}G^{A\mu\nu}\,,$$
$$O_{tG} = y_t g_s (\overline{Q}\sigma^{\mu\nu}T^A t)\tilde{\phi}G^A_{\mu\nu}\,. \qquad (4)$$

The three operators mix under RG flow, $O_{tG}$ mixes into $O_{\phi G}$, and both of them mix into $O_{t\phi}$. Results for the cross sections at 13 TeV are summarised in Table 2 using the notation of Eq. (3). The renormalisation and factorisation scale, EFT scale and PDF uncertainties are also shown. The EFT scale uncertainty is associated with the missing higher order corrections to the operators. It is obtained by computing the EFT cross section at a different EFT scale and then evolving this result taking mixing and running effects into account. A detailed discussion of RG effects and a

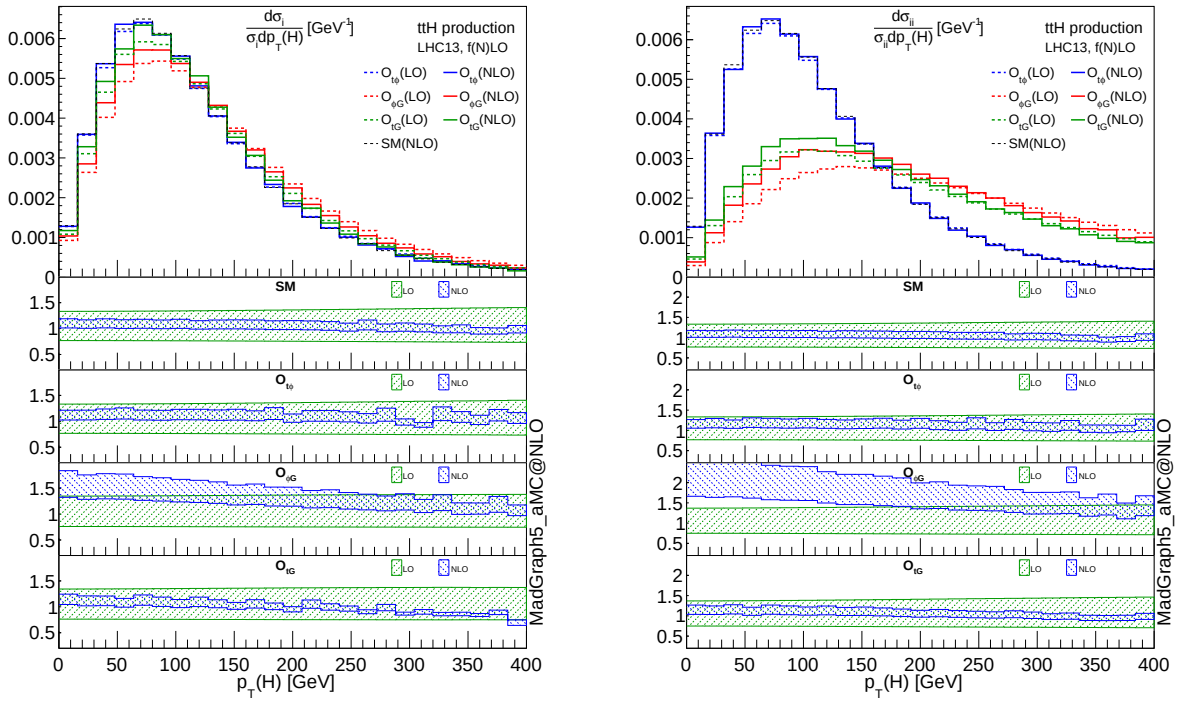


Figure 4: Transverse momentum distributions of the Higgs boson in $t\bar{t}H$ at 13 TeV, normalised. Left: interference contributions from $\sigma_i$. Right: squared contributions $\sigma_{ii}$. SM contributions and individual operator contributions are displayed. Lower panels give the $K$ factors and $\mu_{R,F}$ uncertainties.

comparison between full NLO and RG corrections is presented in [24], demonstrating that RG corrections are not a good approximation of the full NLO result.

Differential distributions can be obtained both at fixed-order and matched to the parton shower. Figure 4 shows the $p_T$ of the Higgs in $t\bar{t}H$ at 13 TeV at LO and NLO (fixed-order), demonstrating different shapes between different operators and non-flat $K$-factors.

Finally a connection between the top and Higgs sectors is drawn by also considering the loop-induced processes $gg \to H$, $pp \to Hj$ and $gg \to HH$ for which predictions at dimension-6 are given for the operators of Eq. (4). The contributions of the chromomagnetic operator ($O_{tG}$) to $Hj$ and $HH$ are obtained for the first time. Current LHC results for single Higgs and $t\bar{t}H$ production and projections for the High Luminocity (HL) LHC can be used to extract current and potential limits on the operator coefficients. An example of a two operator fit is shown in Fig. 5, where the degeneracy between $O_{t\phi}$-$O_{\phi G}$ is broken by considering both single Higgs and $t\bar{t}H$ results. A more detailed discussion is given in [24].

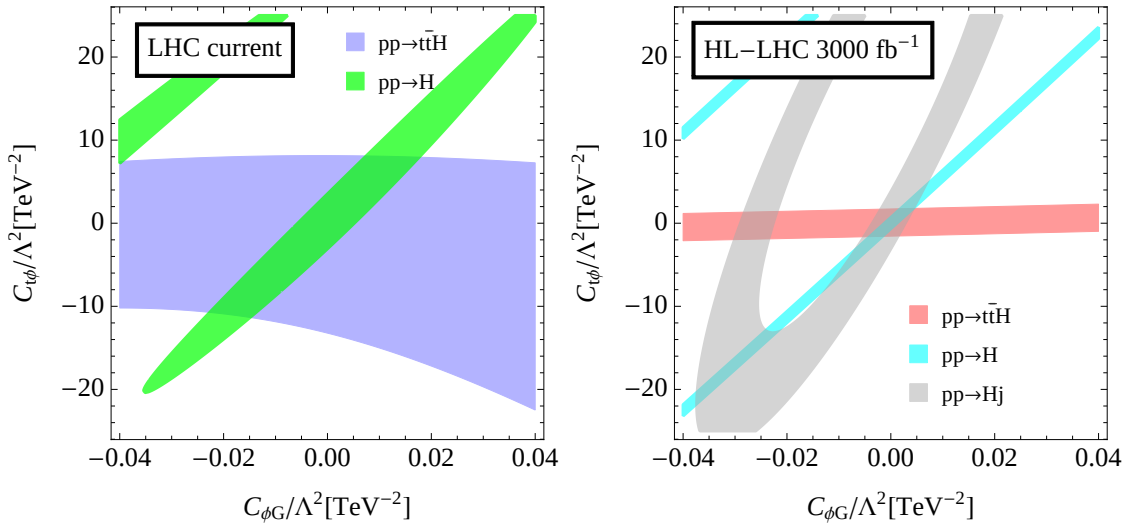


Figure 5: Allowed region in $O_{t\phi}$-$O_{\phi G}$ plane at 95% confidence level. Left: current constraints. Right: future projection at HL-LHC.

# 4 Summary

In these proceedings I summarised the computation of top quark processes, in particular $t\bar{t}V$ and $t\bar{t}H$ in the SMEFT at NLO in QCD within the automated MG5_aMC framework. Results for loop-induced processes can also be extracted in the same setup. These results can be readily used to improve the results of global EFT fits in the top sector.


## ACKNOWLEDGEMENTS

I would like to thank O. B. Bylund, F. Maltoni, I. Tsinikos, and C. Zhang for their collaboration on this work.


# References


[1] W. Beenakker, S. Dittmaier, M. Kramer, B. Plumper, M. Spira and P. M. Zerwas, Nucl. Phys. B **653**, 151 (2003) doi:10.1016/S0550-3213(03)00044-0 [hep-ph/0211352].

[2] S. Dawson, C. Jackson, L. H. Orr, L. Reina and D. Wackeroth, Phys. Rev. D **68**, 034022 (2003) doi:10.1103/PhysRevD.68.034022 [hep-ph/0305087].

[3] R. Frederix, S. Frixione, V. Hirschi, F. Maltoni, R. Pittau and P. Torrielli, Phys. Lett. B **701**, 427 (2011) doi:10.1016/j.physletb.2011.06.012 [arXiv:1104.5613 [hep-ph]].

[4] M. V. Garzelli, A. Kardos, C. G. Papadopoulos and Z. Trocsanyi, Europhys. Lett. **96**, 11001 (2011) doi:10.1209/0295-5075/96/11001 [arXiv:1108.0387 [hep-ph]].

[5] A. Denner and R. Feger, JHEP **1511**, 209 (2015) doi:10.1007/JHEP11(2015)209 [arXiv:1506.07448 [hep-ph]].

[6] S. Frixione, V. Hirschi, D. Pagani, H.-S. Shao and M. Zaro, JHEP **1506**, 184 (2015) doi:10.1007/JHEP06(2015)184 [arXiv:1504.03446 [hep-ph]].

[7] H. B. Hartanto, B. Jager, L. Reina and D. Wackeroth, Phys. Rev. D **91**, no. 9, 094003 (2015) doi:10.1103/PhysRevD.91.094003 [arXiv:1501.04498 [hep-ph]].

[8] M. V. Garzelli, A. Kardos, C. G. Papadopoulos and Z. Trocsanyi, JHEP **1211**, 056 (2012) doi:10.1007/JHEP11(2012)056 [arXiv:1208.2665 [hep-ph]].

[9] A. Kardos and Z. Trócsányi, JHEP **1505**, 090 (2015) doi:10.1007/JHEP05(2015)090 [arXiv:1406.2324 [hep-ph]].

[10] F. Maltoni, D. Pagani and I. Tsinikos, JHEP **1602**, 113 (2016) doi:10.1007/JHEP02(2016)113 [arXiv:1507.05640 [hep-ph]].

[11] C. Zhang and F. Maltoni, Phys. Rev. D **88**, 054005 (2013) doi:10.1103/PhysRevD.88.054005 [arXiv:1305.7386 [hep-ph]].

[12] C. Zhang, Phys. Rev. D **90**, no. 1, 014008 (2014) doi:10.1103/PhysRevD.90.014008 [arXiv:1404.1264 [hep-ph]].

[13] C. Degrande, F. Maltoni, J. Wang and C. Zhang, Phys. Rev. D **91**, 034024 (2015) doi:10.1103/PhysRevD.91.034024 [arXiv:1412.5594 [hep-ph]].

[14] D. Buarque Franzosi and C. Zhang, Phys. Rev. D **91**, no. 11, 114010 (2015) doi:10.1103/PhysRevD.91.114010 [arXiv:1503.08841 [hep-ph]].

[15] C. Zhang, Phys. Rev. Lett. **116**, no. 16, 162002 (2016) doi:10.1103/PhysRevLett.116.162002 [arXiv:1601.06163 [hep-ph]].

[16] A. Buckley, C. Englert, J. Ferrando, D. J. Miller, L. Moore, M. Russell and C. D. White, Phys. Rev. D **92**, no. 9, 091501 (2015) doi:10.1103/PhysRevD.92.091501 [arXiv:1506.08845 [hep-ph]].

[17] A. Buckley, C. Englert, J. Ferrando, D. J. Miller, L. Moore, M. Russell and C. D. White, JHEP **1604**, 015 (2016) doi:10.1007/JHEP04(2016)015 [arXiv:1512.03360 [hep-ph]].

[18] J. Alwall *et al.*, JHEP **1407**, 079 (2014) doi:10.1007/JHEP07(2014)079 [arXiv:1405.0301 [hep-ph]].

[19] A. Alloul, N. D. Christensen, C. Degrande, C. Duhr and B. Fuks, Comput. Phys. Commun. **185**, 2250 (2014) doi:10.1016/j.cpc.2014.04.012 [arXiv:1310.1921 [hep-ph]].

[20] C. Degrande, Comput. Phys. Commun. **197**, 239 (2015) doi:10.1016/j.cpc.2015.08.015 [arXiv:1406.3030 [hep-ph]].

[21] C. Degrande, C. Duhr, B. Fuks, D. Grellscheid, O. Mattelaer and T. Reiter, Comput. Phys. Commun. **183**, 1201 (2012) doi:10.1016/j.cpc.2012.01.022 [arXiv:1108.2040 [hep-ph]].

[22] P. de Aquino, W. Link, F. Maltoni, O. Mattelaer and T. Stelzer, Comput. Phys. Commun. **183**, 2254 (2012) doi:10.1016/j.cpc.2012.05.004 [arXiv:1108.2041 [hep-ph]].

[23] O. Bessidskaia Bylund, F. Maltoni, I. Tsinikos, E. Vryonidou and C. Zhang, JHEP **1605**, 052 (2016) doi:10.1007/JHEP05(2016)052 [arXiv:1601.08193 [hep-ph]].

[24] F. Maltoni, E. Vryonidou and C. Zhang, JHEP **1610**, 123 (2016) doi:10.1007/JHEP10(2016)123 [arXiv:1607.05330 [hep-ph]].

[25] J. A. Aguilar-Saavedra, Nucl. Phys. B **812**, 181 (2009) doi:10.1016/j.nuclphysb.2008.12.012 [arXiv:0811.3842 [hep-ph]].

[26] B. Grzadkowski, M. Iskrzynski, M. Misiak and J. Rosiek, JHEP **1010**, 085 (2010) doi:10.1007/JHEP10(2010)085 [arXiv:1008.4884 [hep-ph]].